IEEE Access
Multidisciplinary | Rapid Review | Open Access Journal

Received January 6, 2020, accepted January 26, 2020, date of publication January 29, 2020, date of current version February 6, 2020.

Digital Object Identifier 10.1109/ACCESS.2020.2970340

Iterative Decision Feedback Equalization Using Online Prediction

SERDAR ŞAHİN[1,2], ANTONIO MARIA CIPRIANO[1], CHARLY POULLIAT[2], AND MARIE-LAURE BOUCHERET[2]

[1]Thales, 92230 Gennevilliers, France
[2]IRIT–ENSEEIHT, Toulouse INP (INPT), CNRS, 31000 Toulouse, France

Corresponding author: Serdar Şahin (serdar.sahin@thalesgroup.com)

ABSTRACT In this article, a new category of soft-input soft-output (SISO) minimum-mean square error (MMSE) finite-impulse response (FIR) decision feedback equalizers (DFEs) with iteration-wise static filters (i.e. iteration variant) is investigated. It has been recently shown that SISO MMSE DFE with dynamic filters (i.e. time-varying) reaches very attractive operating points for high-data rate applications, when compared to alternative turbo-equalizers of the same category, thanks to sequential estimation of data symbols. However the dependence of filters on the feedback incurs high amount of latency and computational costs, hence SISO MMSE DFEs with static filters provide an attractive alternative for computational complexity-performance trade-off. However, the latter category of receivers faces a fundamental design issue on the estimation of the decision feedback reliability for filter computation. To address this issue, a novel approach to decision feedback reliability estimation through online prediction is proposed and applied for SISO FIR DFE with either a posteriori probability (APP) or expectation propagation (EP) based soft feedback. This novel method for filter computation is shown to improve detection performance compared to previously known alternative methods, and finite-length and asymptotic analysis show that DFE with static filters still remains well-suited for high-spectral efficiency applications.

INDEX TERMS Decision feedback equalizers, inter-symbol interference, expectation propagation, semi-analytical receiver abstraction, performance prediction, turbo equalization.

I. INTRODUCTION

Joint detection and decoding through iterative exchange of extrinsic information between a soft-input soft-output (SISO) detector and a SISO decoder can achieve near capacity performance with a well-designed coding scheme. In particular, turbo equalization seeks to provide robust high-throughput links over strongly frequency-selective channels.

However, unlike SISO finite-impulse response (FIR) minimum mean squared error (MMSE) linear equalizers (LE) [2], practical SISO MMSE FIR DFE structures have not been thoroughly investigated, and only gathered attention in recent years [1], [3], [4]. In this article, a novel filter computation approach for such structures is proposed, through a predictive estimation of the decision feedback reliability. In the following, we mainly consider SISO MMSE FIR receiver structures. Although there exists other filter-based equalization techniques in the literature, such as block filter-banks, Kalman smoothers or frequency-domain equalizers (FDE) [5], [6], due to the sliding-window processing, FIR structures are better suited for handling symbol-wise serial decision feedback. This capability will be shown to bring significant performance gain when operating with high order modulations or high code rates.

A widespread and widely accepted nomenclature for categorizing such equalizers has not been established in the literature. In our view, the work in [7] provides an accurate categorization based on the occurrence of SISO adaptive filter updates with prior information. This nomenclature is attractive as it is directly related to the assumptions used for the derivation of the equalizer, and it also gives some insights on both the decoding performance and the computational complexity. Time varying (TV) FIR filters are updated at each single symbol, by fully exploiting prior information, and they are well-suited for doubly-selective channels. However, they have high computational requirements and fast channel estimation and tracking must also be implemented in the receiver. Iteration varying (IV) FIR filters are static inside

The associate editor coordinating the review of this manuscript and approving it for publication was Sabu M. Thampi.

one data block and updated only at the beginning of each turbo iteration, by using the knowledge of overall quality of the feedback, thus reducing the involved computational costs. They are hence excellent candidates for equalization in time-varying channels whose variation is sufficiently slow to be considered static inside one data block (block fading channel model).

The nature of feedback "decisions" (or rather "estimates") also impacts the DFE error-rate performance. Hard decisions can be taken, as in conventional DFE [8], but this results in a significant amount of error propagation and unpredictable behavior [9], unless complex heuristics are used [10]. Alternatively, a widespread category of DFE with soft feedback use a posteriori probability (APP) distributions, due to its relative simplicity and fair performance [3], [4], [11]. Finally, soft feedback based on expectation propagation (EP) [12] improves the performance of TV DFE [1], in addition to being more predictable, due to relatively lowered correlations with the equalized estimates [13].

The design of optimum IV DFE receivers is however non-trivial. Indeed, static filters should depend on the decision feedback reliability, and the decision feedback naturally depends on the filters. As a consequence, there does not exist closed-form expression of the optimal filter due to this non-linear "chicken-and-egg" inter-dependence.

IV DFE proposals in the literature use a variety of sub-optimal heuristics for filter computation [3], [4], [11]. For DFE with hard decisions, the conventional approach is to assume a perfect feedback, causing error propagation and performance degradation in real operation [9]. Using soft APP decisions while still assuming perfect feedback partially mitigates error propagation, as soft symbols' magnitudes scale down with unreliability [14]. The first reference to incorporate APP soft feedback reliability in filter computations is the receiver proposed in [11] for the special case of binary-phase-shift-keying (BPSK) modulation. The direct dependencies between soft symbols and log-likehood ratios (LLRs) for the BPSK constellation enable the use of a tractable density evolution on the APP LLR distribution, given a prior LLR distribution from the decoder. This property is used by the BPSK receiver of [11] to estimate the decision feedback reliability. However, this scheme cannot be directly generalized to high-order constellations; hence [3] proposed a receiver that implements a LE at the first turbo iteration, and then it uses previous turbo iteration's demapper APP LLRs to estimate soft-symbol statistics for IV DFE. Note that this approach is only possible with Gray mapped constellations. More recently, [4] proposed pre-equalization with LE over a few symbols, and then to use APP distribution of these symbols to estimate APP soft-feedback statistics for IV DFE.

Considering the previous developments, our contributions can be summarized as follows:

- An IV DFE with soft APP feedback based on online prediction is formulated. The technique in [11] is extended with models from the field of semi-analytic performance prediction [15]–[17], used both for physical layer abstraction or link layer adaptation.
- A low complexity IV DFE with soft EP-based feedback is proposed, as an IV extension of [1], by removing the bias from predicted APP estimates' reliability.
- A novel approach for estimating soft decision feedback reliability is proposed, based on online binary and symbol-wise semi-analytic performance prediction.
- The accuracy and the convergence of these prediction schemes are evaluated and the performance of IV equalizers are compared. To our knowledge, the accuracy of different IV DFE heuristics is not compared elsewhere, despite their direct impact on DFE error propagation.

The remainder of this paper is organized as follows. Section II presents the system model and the general structure of proposed IV DFE receivers. The involved semi-analytic prediction scheme is developed and analyzed in Section III. Finally, before concluding, the proposed equalizers with online prediction are numerically analyzed in Section IV, in the finite-length and the asymptotic regimes.

Notations: Bold lowercase letters are used for vectors: let $\mathbf{u}$ be a $N \times 1$ vector, then $u_n, n = 1, \ldots, N$ are its entries, unless specified otherwise. Capital bold letters denote matrices: for a $N \times M$ matrix $\mathbf{A}$, $[\mathbf{A}]_{n,:}$ and $[\mathbf{A}]_{:,m}$ respectively denote its n^{th} row and m^{th} column, and $a_{n,m} = [\mathbf{A}]_{n,m}$ is the entry (n, m). $\mathbf{I}_N$ is the $N \times N$ identity matrix, $\mathbf{0}_{N,M}$ and $\mathbf{1}_{N,M}$ are respectively all zeros and all ones $N \times M$ matrices. $\mathbf{e}_n$ is the $N \times 1$ indicator whose only non-zero entry is $e_n = 1$. Operator $\mathbf{Diag}(\mathbf{u})$ denotes the diagonal matrix whose diagonal is defined by $\mathbf{u}$. $\mathbb{R}$, $\mathbb{C}$, and $\mathbb{F}_k$ are respectively real, complex and k^{th} order Galois fields.

Let x and y be two random variables, $\mu_x = \mathbb{E}[x]$ is the expected value, $\sigma_x^2 = \text{Var}[x]$ is the variance and $\sigma_{x,y} = \text{Cov}[x, y]$ is the covariance. The probability of the discrete random variable x taking the value α is $\mathbb{P}[x = \alpha]$. For random vectors $\mathbf{x}$ and $\mathbf{y}$, we define $\boldsymbol{\mu}_\mathbf{x} = \mathbb{E}[\mathbf{x}]$ and covariance matrices $\Sigma_{\mathbf{x},\mathbf{y}} = \mathbf{Cov}[\mathbf{x}, \mathbf{y}]$ and $\Sigma_\mathbf{x} = \mathbf{Cov}[\mathbf{x}, \mathbf{x}]$. $\mathcal{CN}(\mu_x, \sigma_x^2)$ denotes the circularly-symmetric complex Gaussian distribution of mean μ_x and variance σ_x^2. Finally $\mathcal{N}(x; \mu_x, \sigma_x^2)$ and $\mathcal{CN}(x; \mu_x, \sigma_x^2)$ respectively denote the expressions of the probability density functions of the real and the circular-symmetric complex Gaussian distributions.

II. SYSTEM MODEL

A. SINGLE CARRIER BICM TRANSMISSION

Single carrier transmission using a bit-interleaved coded modulation (BICM) scheme is considered.

Let $\mathbf{b} \in \mathbb{F}_2^{K_b}$ be a K_b-bit information packet. $\mathbf{b}$ is encoded and then interleaved into a codeword $\mathbf{d} \in \mathbb{F}_2^{K_d}$. A memoryless modulator φ then maps $\mathbf{d}$ to the symbol block $\mathbf{x} \in \mathcal{X}^K$, where $\mathcal{X}$ is the M^{th} order complex constellation, with zero mean and average power $\sigma_x^2 = 1$, and with $Q = \log_2 M$. The Q-word associated to x_k is denoted $\mathbf{d}_k = [\mathbf{d}]_{Q(k-1)+1:Qk}$, and both $d_{k,q}$ and $\varphi_q^{-1}(x_k)$ denote the value of the q^{th} bit labelling the x_k, i.e. $d_{Q(k-1)+q}$, with $q = 1, \ldots, Q$.

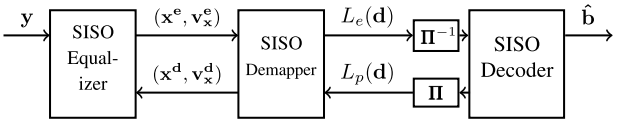

FIGURE 1. Iterative detection and decoding of BICM signals.

We consider an equivalent baseband frequency selective channel with the impulse response $\mathbf{h} = [h_{L-1}, h_{L-2} \dots h_0]$, of delay spread L. Thus the received samples are

$$y_k = \sum_{l=0}^{L-1} h_l x_{k-l} + w_k, \tag{1}$$

for $k = 1, \dots, K$, where the noise w_k is modelled as an additive white Gaussian noise (AWGN), with $\mathcal{CN}(0, \sigma_w^2)$, i.e. a zero mean Gaussian process with variance σ_w^2.

The receiver is assumed to be ideally synchronized in time and frequency, and perfect channel state information is available. We consider an iterative BICM receiver where a SISO channel decoder and a SISO symbol receiver exchange extrinsic information for iterative detection and decoding, as shown in Fig. 1. A priori, extrinsic and a posteriori log likelihood ratios (LLRs) of coded bits $\mathbf{d}$ are respectively denoted $L_p(\cdot)$, $L_e(\cdot)$ and $L(\cdot)$, with respect to the SISO receiver. The considered SISO symbol detector consists of a SISO channel equalizer and a symbol-wise SISO demapper module, as shown in Fig. 1. The latter consits in a soft-output maximum a posteriori (MAP) demapper, and a soft-mapping unit, an APP distribution estimator, and the eventual use of the so-called ''Gaussian division'' operation for computing extrinsic symbol feedback (see discussion below and [1]).

The SISO equalizer computes an estimate x_k^e of x_k, affected by a residual noise of variance $v_{x,k}^e$, whereas the SISO demapper uses these estimates to compute $L_e(\mathbf{d})$, and to deliver soft feedback x_k^d to the equalizer for additional interference cancellation, such that $v_{x,k}^d$ is the variance of residual interference and noise of the feedback (this will be discussed in more detail afterwards).

In short, soft mapper uses LLRs from the decoder to estimate a prior distribution on $x_k = \alpha, \forall \alpha \in \mathcal{X}$

$$\mathcal{P}_k(\alpha) \propto \prod_{q=1}^{Q} e^{-\varphi_q^{-1}(\alpha) L_p(d_{k,q})}. \tag{2}$$

Soft demapper estimates a posteriori symbol distribution

$$\mathcal{D}_k(\alpha) \propto \exp\left(-\frac{|\alpha - x_k^e|^2}{v_{x,k}^e}\right) \mathcal{P}_k(\alpha), \quad \forall \alpha \in \mathcal{X}, \tag{3}$$

which allows computing extrinsic LLRs towards the decoder

$$L_e(d_{k,j}) = \ln \frac{\sum_{\alpha \in \mathcal{X}_j^0} \mathcal{D}_k(\alpha)}{\sum_{\alpha \in \mathcal{X}_j^1} \mathcal{D}_k(\alpha)} - L_p(d_{k,j}), \tag{4}$$

with $\mathcal{X}_j^b = \{\alpha \in \mathcal{X} : \varphi_j^{-1}(x) = b\}$ where $b \in \mathbb{F}_2$.

B. ON SISO FIR DFE STRUCTURES AND PROBLEM STATEMENT

FIR structures are modelled with windowed processes; applying a sliding window $[-N_p, N_d]$ on y_k, we define $\mathbf{y}_k = [y_{k-N_p}, \dots, y_{k+N_d}]^T$. N_p and N_d are respectively the number of pre-cursor and post-cursor samples, and we denote $N \triangleq N_p + N_d + 1$, and $N_p' \triangleq N_p + L - 1$. Then, using the same window on w_k, and $[-N_p', N_d]$ on x_k, we have

$$\mathbf{y}_k = \mathbf{H}\mathbf{x}_k + \mathbf{w}_k, \tag{5}$$

with $\mathbf{H}$ being the $N \times N + L - 1$ Toeplitz matrix generated by the static channel $\mathbf{h}$ with the first row being $[\mathbf{h}, \mathbf{0}_{1,N-1}]$.

Exact TV DFE receivers carry out interference cancellation with anti-causal estimates $\bar{\mathbf{x}}_k^{\mathbf{a}} \triangleq [\bar{x}_k^a, \dots, \bar{x}_{k+N_d}^a]$ and causal estimates $\bar{\mathbf{x}}_k^{\mathbf{c}} \triangleq [\bar{x}_{k-N_p'}^c, \dots, \bar{x}_{k-1}^c]$, with related variances $\bar{\mathbf{v}}_{\mathbf{x},k}^{\text{dfe}} \triangleq [\bar{v}_{x,k-N_p'}^c, \dots, \bar{v}_{x,k-1}^c, \bar{v}_{x,k}^a, \dots, \bar{v}_{x,k+N_d}^a]$. Causal estimates are directly dependent on the values of $(x_k^e, v_{x,k}^e)$ from previous turbo iterations, and they depend on mapping constraints. The equalized estimates are [1]

$$\begin{aligned} x_k^e &= \bar{x}_k^a + \mathbf{f}_k{}^H \mathbf{y}_k \\ &\quad - \mathbf{g}_k^{\mathbf{c}\,H} \bar{\mathbf{x}}_k^{\mathbf{c}} - \mathbf{g}_k^{\mathbf{a}\,H} \bar{\mathbf{x}}_k^{\mathbf{a}} \\ v_{x,k}^e &= 1/\xi_k - \bar{v}_{x,k}^a, \quad \begin{cases} \mathbf{f}_k \triangleq {\Sigma_k}^{-1} \mathbf{h}_0 / \xi_k, \\ \xi_k \triangleq \mathbf{h}_0^H \Sigma_k^{-1} \mathbf{h}_0, \end{cases} \end{aligned} \tag{6}$$

with $\Sigma_k \triangleq \sigma_w^2 \mathbf{I}_N + \mathbf{H}\mathbf{Diag}(\bar{\mathbf{v}}_k^{\text{dfe}})\mathbf{H}^H$, $\mathbf{g}_k^{\mathbf{c}} \triangleq [\mathbf{H}^H \mathbf{f}_k]_{1:N_p'}$, $\mathbf{g}_k^{\mathbf{a}} \triangleq [\mathbf{H}^H \mathbf{f}_k]_{N_p'+1:N_p'+N_d}$ and $\mathbf{h}_0 \triangleq [\mathbf{H}]_{:,N_p'+1}$. In this paper, for numerical results the values of window parameters are taken as $N = 3L + 2$ and $N_d = 2L$.

IV DFE is obtained when $\bar{\mathbf{v}}_k^{\text{dfe}}$ is independent of k, with $\bar{\mathbf{v}}_k^{\text{dfe}} = \bar{\mathbf{v}}^{\text{dfe}}$, all filters being invariant, $\mathbf{f}$, $\mathbf{g}^{\mathbf{c}}$ and $\mathbf{g}^a$, as in [4]:

$$\begin{aligned} x_k^e &= \bar{x}_k^a + \mathbf{f}^H \mathbf{y}_k \\ &\quad - \mathbf{g}^{\mathbf{c}\,H} \bar{\mathbf{x}}_k^{\mathbf{c}} - \mathbf{g}^{\mathbf{a}\,H} \bar{\mathbf{x}}_k^{\mathbf{a}} \\ v_x^e &= 1/\xi - \bar{v}_x^a, \quad \begin{cases} \mathbf{f} \triangleq \Sigma^{-1} \mathbf{h}_0 / \xi, \\ \xi \triangleq \mathbf{h}_0^H \Sigma^{-1} \mathbf{h}_0. \end{cases} \end{aligned} \tag{7}$$

The variances of soft interference cancellation estimates are

$$\bar{\mathbf{v}}_{\mathbf{x}}^{\text{dfe}} = [\bar{v}_x^c \mathbf{1}_{N_p',1}, \bar{v}_x^a \mathbf{1}_{N_d+1,1}], \tag{8}$$

where $\bar{v}_x^a$ and $\bar{v}_x^c$ are respectively the overall reliability of anti-causal and causal estimates. For interference cancellation, the set of anti-causal estimates are available before equalization, and an accurate estimate of their reliability is given by the least-squares estimation; $\bar{v}_x^a = K^{-1} \sum_{k=0}^{K-1} \bar{v}_{x,k}^a$. In most SISO DFE structures, the anti-causal estimates are the prior estimates given by the decoder[1]: $x_k^p \triangleq \mathbb{E}_{\mathcal{P}_k}[x_k]$, $v_{x,k}^p \triangleq \text{Var}_{\mathcal{P}_k}[x_k]$.

As stated in the introduction, the core of the problem lies in the computation of $\bar{v}_x^c$. A simple, but inaccurate solution to this is the ''perfect decision assumption'': $\bar{x}_k^c$ are all assumed

[1]However, note that in the self-iterated SISO DFE of [1], the anti-causal estimates are the causal estimates of previous iterations.

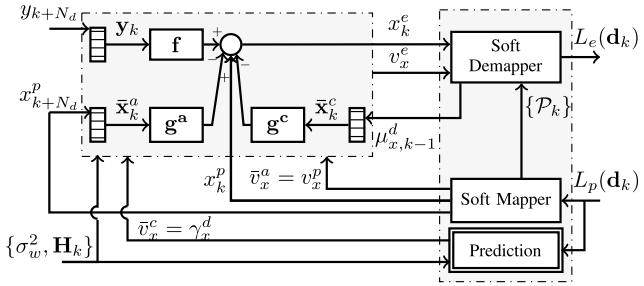

FIGURE 2. Soft-input soft-output IV DFE APP structure.

to be equal to x_k, yielding $\bar{v}_x^c = 0$. This approach is sufficient at high SNR operating points, but as shown in [1], [9], it degrades performance in moderately or severely selective channels.

Hence, with these notations, this paper's main objective is to evaluate novel prediction methods to compute $\bar{x}_k^c$ for optimizing the inter-symbol interference (ISI) mitigation performance of IV DFE. In the following, the cases of IV DFE based on APP-based soft feedback (see Fig. 2), and EP-based soft feedback (see Fig. 3) will be discussed.

C. APP SOFT FEEDBACK COMPUTATION

A common approach to compute soft feedback for DFE is to use APP estimates, as in IV structures of [3], [4], [11]. Derivation of a DFE APP for TV FIR is available in [1].

These soft estimates are given by the mean and the variance of the posterior symbol distribution $\mathcal{D}_k$, given in Eq. (3). We denote

$$\begin{aligned} \mu_k^d &\triangleq \mathbb{E}_{\mathcal{D}_k}[x_k] = \textstyle\sum_{\alpha\in\mathcal{X}} \alpha \mathcal{D}_k(\alpha), \\ \gamma_{x,k}^d &\triangleq \mathrm{Var}_{\mathcal{D}_k}[x_k] = \textstyle\sum_{\alpha\in\mathcal{X}} |\alpha|^2 \mathcal{D}_k(\alpha) - |\mu_k^d|^2. \end{aligned} \quad (9)$$

For the IV DFE APP filter computation, an invariant variance γ_x^d is needed, as with the causal reliability $\bar{v}_x^c$. Unlike the anti-causal reliability, γ_x^d cannot be estimated using the causal estimates $(\bar{x}_k^c, \bar{v}_{x,k}^c) = (\mu_k^d, \gamma_{x,k}^d)$, as causal estimates are only available once the filter is computed, and the equalization is being carried out. Thus, a predictive estimation is required. This receiver corresponds to the Fig. 2, with $\bar{v}_x^c = \gamma_x^d$.

D. PREDICTIVE EP-BASED SOFT FEEDBACK COMPUTATION

In [1], an expectation propagation (EP) based soft feedback is used within a TV DFE which proved to bring several performance improvements. Unlike APP estimates, EP-based estimates carry only the extrinsic information brought by the demapper, and prevents DFE from relying on its own bias, and improves the asymptotic predictability of the receiver. For TV DFE, these estimates are obtained by the division of two Gaussian PDFs, which yields another Gaussian PDF with mean and variance given by

$$x_k^d = \frac{\mu_k^d v_x^e - x_k^e \gamma_{x,k}^d}{v_x^e - \gamma_{x,k}^d}, \quad \text{and,} \quad v_{x,k}^d = \frac{v_x^e \gamma_{x,k}^d}{v_x^e - \gamma_{x,k}^d}. \quad (10)$$

For the sake of simplicity, this operation is referred to as "Gaussian division".

For IV DFE EP structure, this feedback is not adapted, as the invariant filter is unable to adapt its coefficients to handle the strong variations of $v_{x,k}^d$, which depends on the instantaneous APP variance $\gamma_{x,k}^d$. Hence we propose to use a feedback based on overall APP reliability, with

$$x_k^d = \frac{\mu_k^d v_x^e - x_k^e \gamma_x^d}{v_x^e - \gamma_x^d}, \quad \text{and,} \quad v_{x,k}^d = \frac{v_x^e \gamma_x^d}{v_x^e - \gamma_x^d}, \quad (11)$$

where a predicted invariant APP variance γ_x^d is used to generate the feedback. Moreover EP-based estimates have an invariant variance, i.e. $v_x^d \triangleq v_{x,k}^d, \forall k$, as the causal reliability is directly related to the predicted APP variance. The receiver based on this structure is illustrated in the Fig. 3, with $\bar{v}_x^c = v_x^d$.

III. SEMI-ANALYTIC ABSTRACTION OF SISO FIR DFE

In this section, a prediction model for the turbo DFE structure of Equation (7) is exposed, without loss of generality, for the case where anti-causal estimates are given by decoder's extrinsic LLRs, i.e. $\bar{v}_x^a = v_x^p$. Such models are usually used for handling physical layer link quality prediction that is necessary to enable link adaptation with low computational complexity. The originality is that, in our context, it will be exploited for online estimation of the reliability of causal estimates for SISO DFE filter computation.

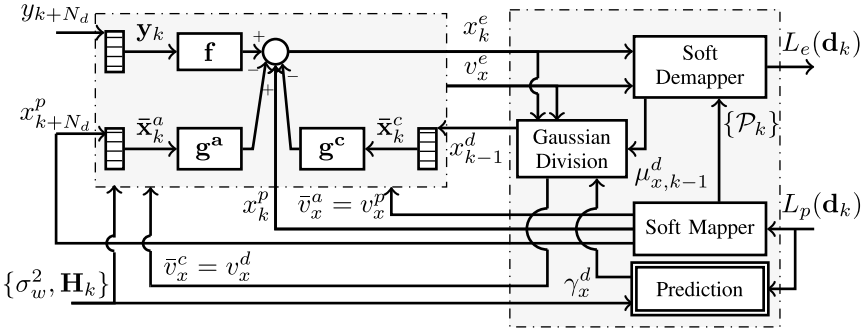

FIGURE 3. Soft-input soft-output IV DFE EP structure.

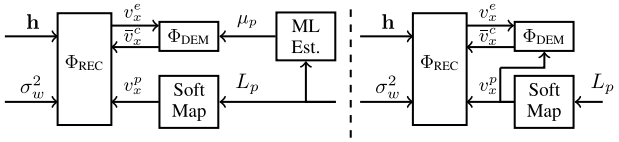

FIGURE 4. Block diagrams for bit-wise (left) and symbol-wise (right) causal reliability prediction schemes.

A. GENERAL STRUCTURE AND ANALYTICAL EQUALIZER MODEL

SISO DFE is modelled with two independent components; an analytical model for the equalizer, and a numerical model for the soft demapper. Unlike asymptotic transfer models ($K \to +\infty$) used in extrinsic information transfer (EXIT) analysis [18], finite-length transfer models are used for characterizing the demapper, as prior works on performance prediction noted their positive impact on accuracy [15], [16].

Following Eq. (7), the IV DFE-IC output reliability v_x^e is modelled by a function ϕ_{REC} as

$$\begin{aligned} v_x^e &= \phi_{\text{REC}}(\sigma_w^2, \mathbf{h}, v_x^p, \bar{v}_x^c) \\ &\triangleq \left(\mathbf{h}_0^H \left[\sigma_w^2 \mathbf{I}_N + \mathbf{H}\mathbf{Diag}(\bar{\mathbf{v}}_{\mathbf{x}}^{\text{dfe}})\mathbf{H}^H\right]^{-1} \mathbf{h}_0\right)^{-1} - v_x^p, \end{aligned} \quad (12)$$

where $\bar{\mathbf{v}}_{\mathbf{x}}^{\text{dfe}}$ is given by Eq. (8), with $\bar{v}_x^a = v_x^p$. This function is strictly increasing with $\bar{v}_x^c \in [0, \sigma_x^2]$.

As an analytical model is unavailable for characterizing the demapper, it is modelled with a look-up table (LUT) ϕ_{DEM}, given by

$$\bar{v}_x^c = \phi_{\text{DEM}}(v_x^e, \cdot), \quad (13)$$

where $\bar{v}_x^c$ is the expected value of causal estimates' variance, taken over realizations of the channel noise, the equalizer outputs and the prior LLRs. The second argument '$\cdot$' in Equation (13) models prior information, and the exact nature of the argument depends on the selected prediction approach. Improvements proposed in the upcoming subsection concern this module.

Since equalizer and demapper iteratively exchange reliabilities, the two functions representing their model must be composed to yield a recursive equation on $\bar{v}_x^c$. Hence by using $n = 0, \ldots, N_{\text{pred}}$ for indexing recursions, we have

$$\bar{v}_x^c[n+1] = \phi_{\text{DEM}}(\phi_{\text{REC}}(\sigma_w^2, \mathbf{h}, v_x^p, \bar{v}_x^c[n]), \cdot) \triangleq f_{\text{pred}}(\bar{v}_x^c[n]). \quad (14)$$

If f_{pred} admits a unique fixed-point on $\bar{v}_x^c$, then the desired predicted reliability estimate is this fixed-point. Moreover, the optimality of IV DFE-IC strongly depends on $\bar{v}_x^c$ and hence on the accuracy of Φ_{DEM}.

Fig. 4 illustrates reliability prediction structures with the two semi-analytical models that will be introduced below.

B. NUMERICAL DEMAPPING MODELS FOR APP/EP

Modelling the demapper with prior information is challenging due to its highly non-linear behavior, and due to strong simplifying assumptions. The main focus of the study is the model of the posterior symbol distribution's variance γ_x^d. This quantity is used for both DFE with APP feedback (see Subsection II-C) and DFE with EP feedback (see analytical link with v_x^d in (11)).

1) MUTUAL INFORMATION BASED PREDICTION (BIT-WISE)

In the BPSK receiver of [11], a prediction scheme is considered, assuming input/output LLRs of the demapper to be consistent Gaussian, i.e. $L_{(\cdot)}(d_{k,q}) \sim \mathcal{N}(\bar{d}_{k,q}\mu_{(\cdot)}, 2\mu_{(\cdot)})$, where $\bar{d}_{k,q} = 1 - 2d_{k,q}$, and where $(\cdot)$ is p, e or void, depending on concerned LLRs. Using a semi-analytical density evolution, parameter μ_e of extrinsic LLRs is predicted using μ_p. The parameter $\mu_{(\cdot)}$ is bijectively linked to the average mutual information (MI) between LLRs and the associated coded bits, usable for binary prediction as in [15]. Hence using such formalism, the approach of [11] can be extended to any constellation and mapping.

More specifically, the demapper behaviour is numerically integrated for each $\gamma_{x,k}^d$, $k = 1, \ldots, K$, under the assumption that prior LLRs are consistent Gaussian with the parameter μ_p, and the assumption that the residual ISI and noise affecting the equalized symbols x_k^e are Gaussian-distributed, i.e. $x_k^e \sim \mathcal{CN}(x_k, v_x^e)$. Hence with these conditions, a LUT on μ_p and v_x^e is built with

$$\bar{v}_x^c = \phi_{\text{DEM}}(v_x^e, \mu_p) \triangleq \frac{1}{K}\sum_{k=1}^{K} \mathbb{E}_{\mathbf{L_p}, x^e}[\bar{v}_{x,k}^c], \quad (15)$$

where $\bar{v}_x^c$ is the variance of residual error on APP/EP soft symbols and the priors' parameter μ_p is measured with a maximum-likelihood (ML) estimator (see Fig. 4, left)

$$\mu_p \approx \sqrt{1 + \sum_{k=1}^{K}\sum_{q=1}^{Q} |L_p(d_{k,q})|^2} - 1. \quad (16)$$

In the case of APP feedback, i.e. for $\bar{v}_{x,k}^c = \gamma_{x,k}^d$, the expectation in Equation (15) becomes

$$\begin{aligned} &\mathbb{E}_{\mathbf{L_p}, x^e}[\gamma_{x,k}^d] \\ &= \frac{1}{M}\sum_{x_k \in \mathcal{X}} \text{Var}\left[\mathcal{D}(x_k, x_k^e, \mathbf{L_{p,}}_k)\right] \\ &\quad \times \mathcal{CN}(x_k^e; x_k, v_x^e) \textstyle\prod_{q=1}^{Q} \mathcal{N}(L_{p,k,q}; \bar{\varphi}_q^{-1}(x_k)\mu_p, 2\mu_p) \end{aligned} \quad (17)$$

where the APP probability mass function of a dummy symbol $x \in \mathcal{X}$ is given by

$$\mathcal{D}(x, x^e, \mathbf{L_p}) \triangleq \frac{1}{Z} \exp\left(-\frac{|x - x^e|^2}{v^e} - \sum_{q=1}^{Q} \varphi_q^{-1}(x^e) L_{p,q}\right), \quad (18)$$

with Z being the normalization constant such that $\sum_{x \in \mathcal{X}} \mathcal{D}(x, x^e, \mathbf{L_p}) = 1$. Moreover, considering the EP feedback's analytical expression in Equation (11), we have

$$\mathbb{E}_{\mathbf{L_p}, x^e}[\gamma_{x,k}^d] = \left(\left(\frac{1}{K}\sum_{k=1}^{K} \mathbb{E}_{\mathbf{L_p}, x^e}[\gamma_{x,k}^d]\right)^{-1} - \frac{1}{v_x^e}\right)^{-1}. \quad (19)$$

The binary prediction scheme above appeared to yield too optimistic estimates in [11], and instead *Lopes et al.* resorted to obtain μ_e and μ_p through BPSK channel estimators, which circumvents consistent Gaussian LLR approximation.

More specifically, this problem ensues from well known issues with regards to performance prediction of turbo iterative systems, for which the consistent Gaussian approximation of LLRs was shown to be only accurate at the zeroth turbo-iteration, and in the asymptotic limit. Otherwise inaccurate estimates propagate across turbo iterations due to the internal non-linear dynamics of channel decoding [19]. To overcome this prediction bias, prediction based on a two-parameter LLRs' model has been shown to be much more accurate [20]. Such models consider $L_{(\cdot)}(d_{k,q}) \sim \mathcal{N}(\bar{d}_{k,q}\mu_{(\cdot)}, \eta_{(\cdot)}\mu_{(\cdot)})$, where $\eta_{(\cdot)}$ is no longer 2. The ML estimator used for measuring μ_p in the binary prediction is very sensitive to η_p, which is the reason why the binary prediction is not robust enough in practice.

2) PRIOR VARIANCE BASED PREDICTION (SYMBOL-WISE)

For our context, two-parameter models are too complex as they require expensive online parameter estimators to get both μ_p and η_p. Hence, a single-parameter demapper model with reasonable estimation complexity has been preferred. We searched for the parameter which is the least sensitive to the variations of prior LLRs' variance-to-mean ratio η_p.

Following a thorough and almost exhaustive study of the different alternative parameters for tracking evolution of $\bar{v}_x^c$, anti-causal variance v_x^p has been found to be sensitive to the changes on η_p, very similarly to $\bar{v}_x^c$, with the advantage of v_x^p being directly computable online using a simple least-squares estimation. Hence, we propose the following LUT

$$\bar{v}_x^c = \phi_{\text{DEM}}(v_x^e, v_x^p), \quad \begin{cases} \bar{v}_x^c \triangleq K^{-1} \sum_{k=1}^{K} \mathbb{E}_{\mathbf{L_p}, x^e}[\bar{v}_{x,k}^c], \\ v_x^p \triangleq K^{-1} \sum_{k=1}^{K} \mathbb{E}_{\mathbf{L_p}}[v_{x,k}^p], \end{cases} \tag{20}$$

where both input v_x^p and output $\bar{v}_x^c$ are numerically integrated using prior LLRs generated for a fixed value of η_p. However, as η_p cannot be accurately measured online, the conventional consistent approximation [15] is kept ($\eta_p = 2$). In the following, we will assess its impact on the prediction accuracy.

3) ROBUSTNESS OF DEMAPPER PREDICTION

The sensitivity of the considered prediction schemes to variations in η_p is evaluated. This aspect is important for characterizing the robustness of iterative receiver prediction schemes, as the hypothesis $\eta_p = 2$, used for LUT generation, is only true at the initial turbo-iteration and then it varies [19].

An AWGN channel is simulated with blocks of 16-QAM symbols with $K = 1024$, to emulate the output x^e of the equalizer, for v^e varying from -15 to 15 dB, along with Gaussian-distributed prior LLRs generated with prior MI I_A varying from 0 to 1 bit (and hence determining μ_p), with η_p varying from 1 to 3. The average mean squared error (MSE) between the predicted causal covariance and true causal covariance is measured, and plotted in Fig. 5. The left side of the figure provides results for APP feedback, and the right side for EP-based feedback. The binary approach is seen to be severely impacted by the changes in η_p, whereas the symbol-wise approach, although not perfect, remains more robust. Considerable differences are seen at low to medium SNR for high prior information, which suggests that symbol-wise schemes would have an advantage at the decoding threshold in asymptotic behaviour, i.e. when a high number of turbo-iterations are used. Oppositely, without any turbo-iteration, both schemes would perform identically.

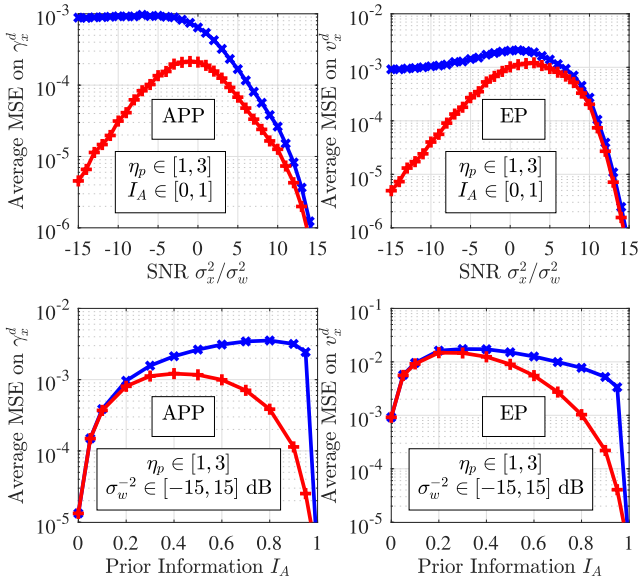

FIGURE 5. Mean-square error on the prediction quality of the binary (blue, ×) and symbol-wise (red, +) schemes.

C. CONVERGENCE ANALYSIS

The convergence of the proposed iterative semi-analytical prediction schemes could be assessed formally through fixed-point analysis of Eq. (14). However, due to the untractable non-linear expression of Φ_{DEM}, an analytic approach is not possible, and we resort to numerical evaluations. In the following, the convergence of the symbol-wise prediction scheme is evaluated.

Numerical evaluations of the proposed f_{pred} show that we can reasonably conjecture that this function is continuous on the interval $[0, +\infty[$, with a Lipschitz constant strictly less than one, for all $\sigma_w^2 \geq 0$ and $0 \leq v_x^p \leq \sigma_x^2$. This ensures that Eq. (14) reaches a unique fixed-point $\bar{v}_x^c \in [0, +\infty[$ for any initial guess. This conjecture has been checked for various channels $\mathbf{h}$, and Fig. 6 plots f_{pred} for the Proakis-C channel ($\mathbf{h} = [1, 2, 3, 2, 1]/\sqrt{19}$), using the symbol-wise demapper model for the Gray-mapped 16-QAM constellation.

The convergence speed of the prediction scheme is also evaluated numerically in order to determine optimal parameters of the algorithm. Indeed, the fixed-point $\bar{v}_x^c = \bar{v}_x^c[\infty]$ is reached more or less quickly depending on if the initial value $\bar{v}_x^c[0]$ is close to $\bar{v}_x^c[\infty]$.

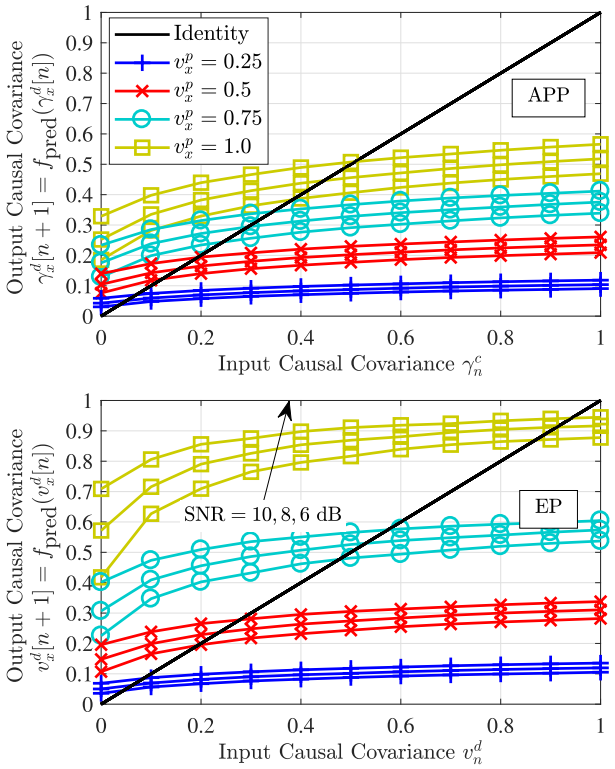

FIGURE 6. Fixed-points of the symbol-wise f_{pred} for SNR decreasing from 10 to 6 dB, for each value of prior reliability.

In particular, due to the near flat evolution of f_{pred} for $\bar{v}_x^c$ close to $\sigma_x^2 = 1$, initializing with $\bar{v}_x^c[0] = 1$ results in fast convergence at low SNRs, and high anti-causal covariance, but slow convergence otherwise. Oppositely with $\bar{v}_x^c[0] = 0$ faster convergence is achieved for high SNRs and low anti-causal covariance. This behaviour is illustrated for Proakis-C 16-QAM APP covariance in Figure 7.

We propose to use the heuristic $\bar{v}_x^c[0] = \min(1, \sigma_w)$, when $v_x^p > 0.5$, and otherwise using $\bar{v}_x^c[0] = 0$ is preferable for faster convergence. This serves as a convergence accelerating heuristic, by making a compromise on prediction accuracy trade-off between highly reliable feedback, and poor quality feedback. The use of the standard deviation of the AWGN noise σ_w appears experimentally to yield desirable initial values, when the channel is normalized, as illustrated with dashed curves in Figure 7.

IV. NUMERICAL RESULTS

A. UNCODED EQUALIZATION BEHAVIOUR

In this paragraph, the uncoded finite-length behaviour of the proposed IV DFE with online prediction is evaluated. Exact TV DFE counterparts are used as lower-bound references on bit-error rate (BER), to assess the prediction accuracy. Note IV FIR receivers might outperform TV FIRs in some cases [21], as the latter are more sensitive to the convergence errors committed by the SISO decoder.

Block transmission in Proakis C channel is considered with $K = 256$ and with QPSK, 8-PSK and 16-QAM constellations. In Fig. 8, BER of TV DFE with APP and EP feedback are compared to the proposed predictive IV implementations. IV DFE converges towards the curve of TV counterparts, especially at high SNR, but it is seen that a gap remains at medium BER for some constellations, due to dynamic filtering capabilities of TV receivers. EP feedback is shown to be mostly equivalent to APP feedback in this uncoded use case, but at high BER, EP has an advantage over APP both for TV and IV receivers, which suggests that improved decoding thresholds can be obtained with channel coding.

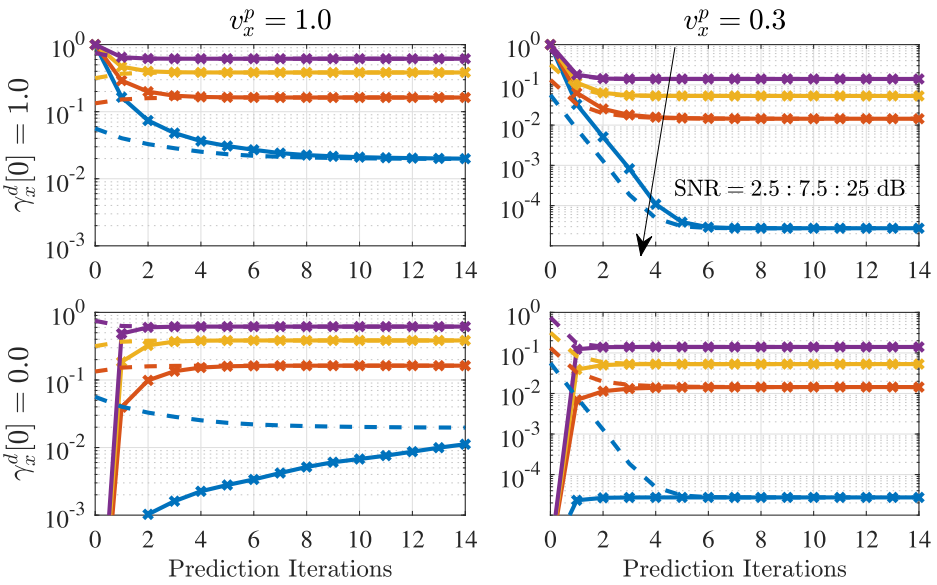

FIGURE 7. Evolution of the predicted APP covariance $\gamma_x^d[n+1] = f_{\text{pred}}(\gamma_x^d[n])$, with solid curves with markers for the initial value with $\gamma_x^d[0] = 0$ or 1 (as per axis on left) and dashed curves for the proposed heuristic ($\gamma_x^d[0] = \min(1, \sigma_w)$). Plot colors are for SNR varying from 2.5 to 25 dB, with 7.5 dB steps.

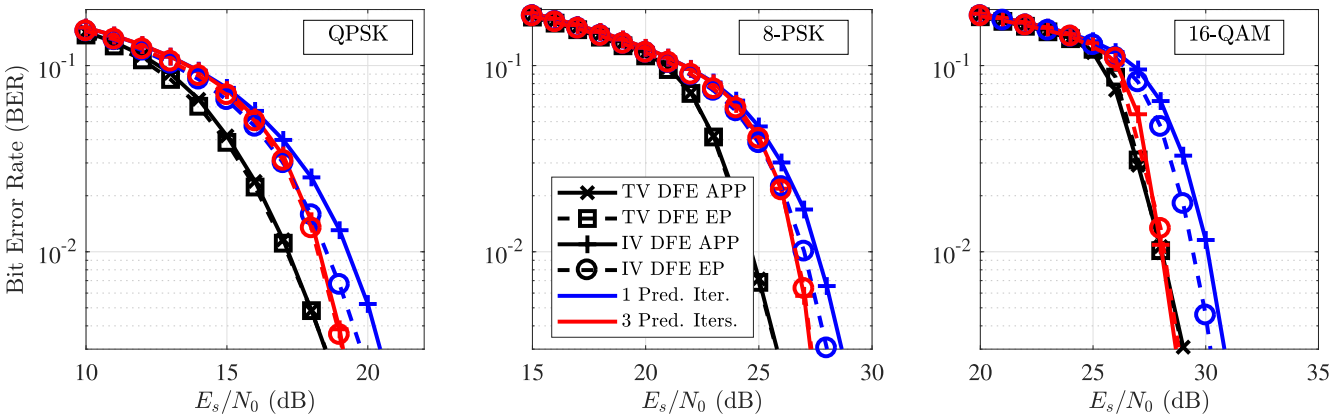

FIGURE 8. Uncoded bit-error rate (BER) performance of proposed predictive IV DFEs.

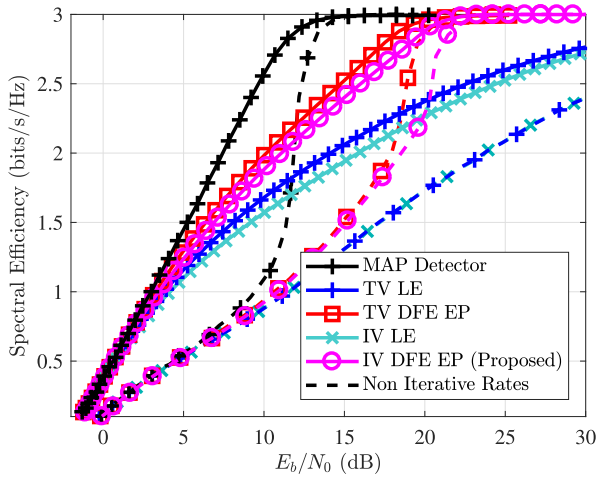

FIGURE 9. Achievable rates of FIR receivers for 8-PSK in Proakis C channel.

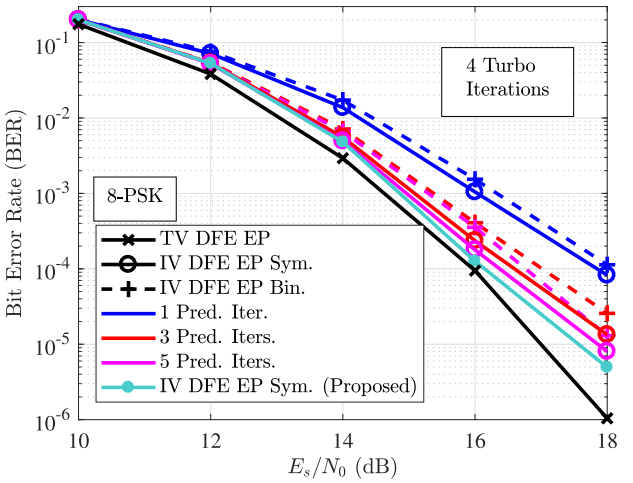

FIGURE 10. Rate-1/2 coded BER with proposed binary and symbol-wise prediction.

B. ON THE OPERATING REGIONS OF FIR RECEIVERS

A previous work on TV FIR turbo equalizers concluded that TV DFE significantly outperforms TV LE at high data rates [1], whereas TV LE remains preferable at very low rates, as it achieves same performance with less complexity. In the following, the asymptotic behaviour and the computational complexity of the proposed receiver along with IV FIRs is evaluated in a similar manner.

Through the extrinsic information transfer (EXIT) analysis of a SISO module, a mutual information (MI) based transfer function model, $I_E = \mathcal{T}_R(I_A, \mathbf{h}, \sigma_w^2)$ is obtained [18], where I_A and I_E denote respectively the MI between coded bits and the prior LLRs and the extrinsic LLRs.

EXIT functions notably allow to numerically predict the achievable rates of SISO receivers, through the area theorem of EXIT charts [22]. Indeed, MAP detector's EXIT chart's area yields an accurate prediction of the channel symmetric information rate (SIR) [23], the highest possible transmission rate for practical constellations, without channel knowledge at the transmitter. However, for approximate receivers which violate the extrinsic message principle of turbo detection, the rates predicted by EXIT can be too optimistic (e.g. SIR of APP DFE appears to surpass MAP, which is impossible). This has been observed for APP-based receivers in [1], [13], but the EP-based DFE does not suffer from this phenomenon. Hence in the following, the proposed predictive EP-based IV DFE is evaluated.

IV DFE EP with symbol-wise prediction scheme is used for 8-PSK transmissions in the Proakis C channel, and numerically obtained achievable rates are plotted in solid lines in Fig. 9. Dotted plots illustrate the achievable rates without turbo-iterations, for each receiver. IV receivers are shown to follow the behaviour of their TV counterpart within a gap of about 0.1 bits/s/Hz for both LE and DFE, but IV DFE still keep a significant upper hand over TV LE at medium and high spectral efficiency operating points. Using IV FIR receivers to operate at a given rate requires about 1.5 dB more energy than TV FIR, but with significant complexity savings.

Approximate computational complexity per turbo-iteration of considered FIR receivers is given in the Table 1. TV LE

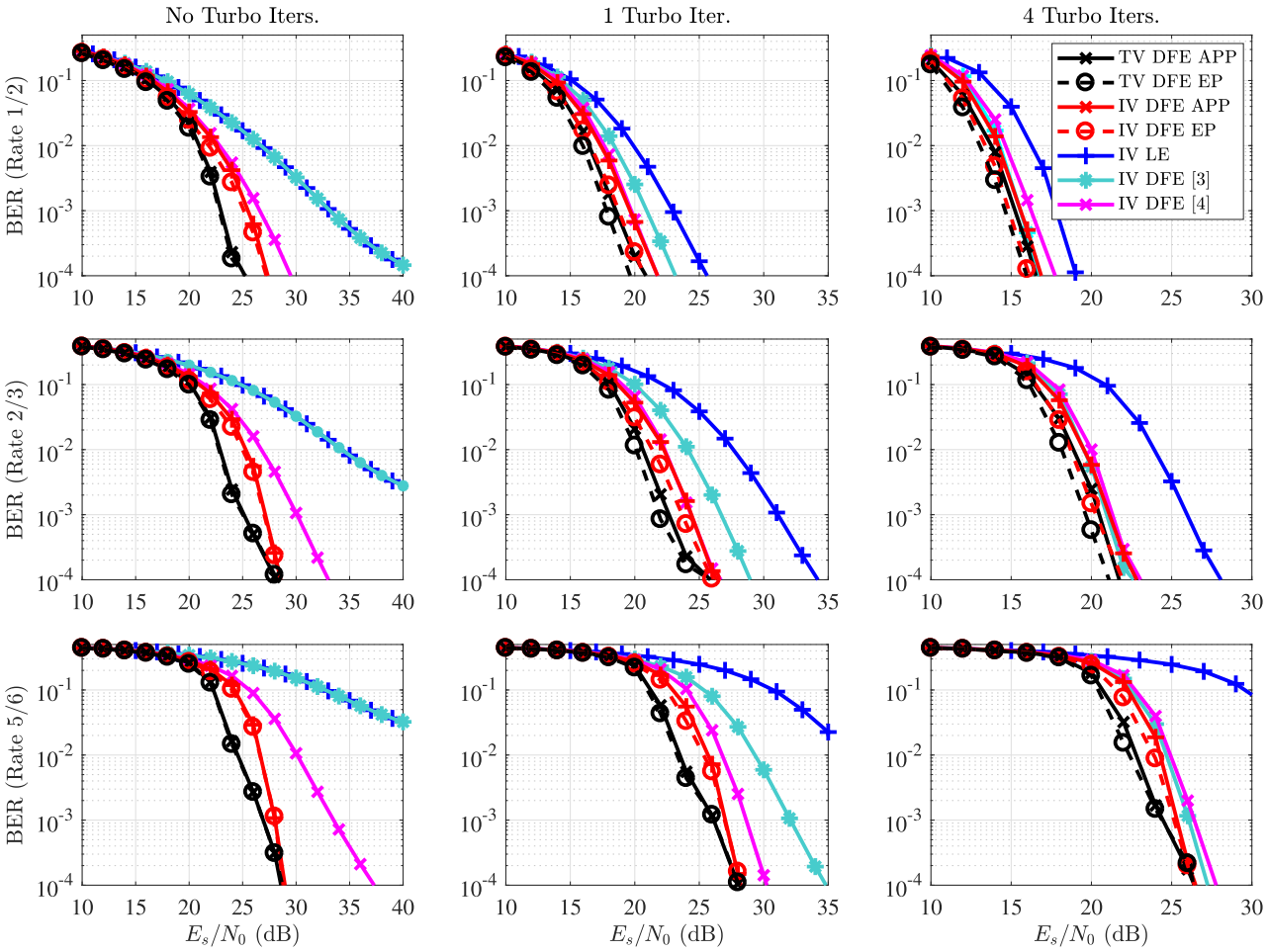

FIGURE 11. Coded 8-PSK bit-error rate (BER) performance comparison of turbo FIR receivers across turbo-iterations for different code rates.

TABLE 1. Computational complexity of FIR receivers.

Structure	Filter Computation	Filtering and Detection
TV LE	$K(5L^3+56L^2)$	$K(25L+(11+3q)M)$
TV DFE	$K(5L^3+71L^2)$	$K(25L+(18+3q)M)$
IV LE	$(6L^3+28L^2)$	$K(25L+(11+3q)M)$
IV DFE	$(N_{\text{pred}}+1)(6L^3+34L^2)$	$K(25L+(18+3q)M)$

and DFE receivers use the reduced-complexity TV matrix inversion algorithms in [1], and IV receivers exploit Cholesky decomposition for matrix inversion. The filter computation cost of the proposed IV DFE increases linearly with the number of prediction iterations N_{pred}.

C. FINITE-LENGTH FINITE-IMPULSE RESPONSE (FIR) TURBO-EQUALIZATION PERFORMANCE

In this section, the prediction accuracy is assessed for transmissions encoded with non-recursive non-systematic convolutional code (NRNSCC) of polynomial $[7, 5]_8$.

First, the impact of choosing a symbol-wise or a binary prediction scheme is assessed through finite-length BER evaluations. The block size is kept at $K = 256$, similarly to the uncoded case, and a MAP decoder based on the BCJR algorithm is used as a SISO decoder [24]. Fig. 10 shows the case of the EP-based feedback with 8-PSK, and the use of symbol-wise prediction is shown to accelerate convergence of the IV DFE performance towards TV DFE [1].

However, despite the improvements brought by the symbol-wise prediction, covariance estimations tend to be too optimistic for high prior information at high SNRs (following 1 or 2 turbo iterations, above 15 dB), and degrade BER performance. A similar observation was made for the semi-analytic prediction of turbo linear MMSE receivers in [25], where a calibration mechanism is applied to correct the predicted prior covariance with a multiplicative penalty factor. After some ad hoc optimization, this scheme yields more pessimistic predictions that ends up improving the BER prediction accuracy.

Here, a related mechanism is adapted to the proposed online prediction. To avoid over-estimation of the causal covariance, the anti-causal covariance can be exploited to derive a "lower-bound" to estimated causal covariances. Empirically, turbo detection systems bring most of the

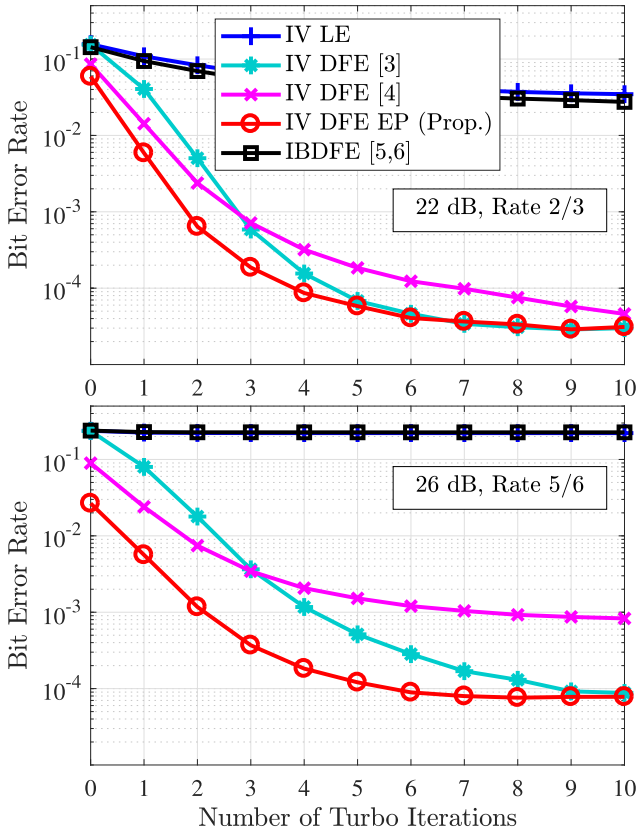

FIGURE 12. BER of the proposed receivers versus turbo-iterations for 8-PSK in Proakis C channel.

improvements at the initial iterations, hence the improvements after a certain number of iterations can no longer be substantial. Thus, after some trial-and-error tests, we have selected the predicted causal covariance $\bar{v}_x^c$ of the current turbo iteration to be modified with the heuristic $\bar{v}_x^c = \max(\bar{v}_x^c, \beta \bar{v}_x^a)$, with $0 < \beta \leq 1$.

The proposed heuristic is integrated with the symbol-wise prediction, with 3 prediction iterations and $\beta = 0.2$, and the IV DFE-EP performance is displayed in turquoise in Fig. 10.

Finally, to compare our proposal to the prior work and to evaluate its behavior in different operating regimes, the previously used rate-1/2 encoding with NRNSCC $[7, 5]_8$ is punctured to get rate-2/3 encoding with [11; 01] puncturing pattern and rate-5/6 encoding with [10001; 01111] puncturing pattern. The BER performance of the proposed IV DFE APP and IV DFE EP receivers are shown in red in Fig. 11, for 8-PSK transmissions in Proakis C channel, with above mentioned codes of rate 1/2, 2/3 and 5/6, and for 0, 1 and 4 turbo-iterations. Proposed predictive IV DFE receivers use symbol-wise prediction with 3 iterations, and the heuristic parameter is $\beta = 0.2$. IV DFE APP significantly outperforms other APP-based DFE receivers when there are no turbo iterations, as this is the operating point where the prediction scheme is the most accurate. In Figure 12, the evolution of BER is plotted as the number of turbo-iterations increases. During intermediary iterations of the rate 2/3 system, previous works of Tao [4] and Lou and Xiao [3] close most

TABLE 2. Computational complexity of FDE.

Structure	Filter Computation	Filtering and Detection
IBDFE	K $(9\log_2 K + 12)$	$K(18\log_2 K + 5$ $+(11+3Q)M)$

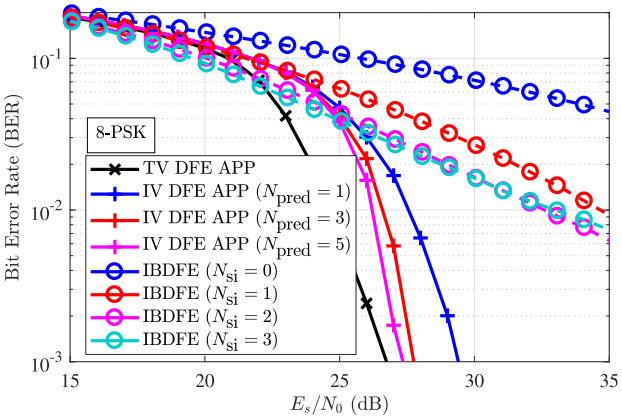

FIGURE 13. BER comparison vs. FDE in uncoded Proakis C.

of the gap of iteration zero, with the receiver of [3] slowly converging to the same limit as the proposed receiver. At high rate systems (rate 5/6) the gap between them and our proposal increases, even for 4 turbo-iterations, and from Figure 12 it is seen that the receiver of [4] cannot converge to the same asymptotic limits, probably due to the usage of only a few samples for covariance estimation heuristic. The use of EP-feedback instead of APP does not bring significant improvement for high-rates, or without turbo-iterations, but at medium and low rates, it allows for an additional asymptotic gain over 0.5 dB. However, the predictability of the EP feedback over a wider set of configurations makes it a more attractive solution.

D. COMPARISON WITH LOW-COMPLEXITY FREQUENCY DOMAIN RECEIVERS

In this section the proposed sliding-window FIR turbo IV DFE is compared with the state-of-the-art turbo FDE techniques, belonging to the different category of block equalizers. FDE are known to be attractive for practical receivers, as they enable low-complexity equalization through the use of fast Fourier transform (FFT).

In particular, turbo equalization concept has been originally extended for FDE in [6], and then an original FDE, called iterative-block DFE (IBDFE), with APP-based feedback from a decision device was proposed in [5], [26]. For uncoded systems IBDFE achieves considerable performance gains, and its coded extension coincides with the turbo FDE [5]. The estimated computational complexity of this structure, per turbo-iteration, is given in Table 2.

Although this structure has quasi-linear computational complexity, the transmitted signal has an increased overhead, due to the use of cyclic prefixing, or zero-padding, needed

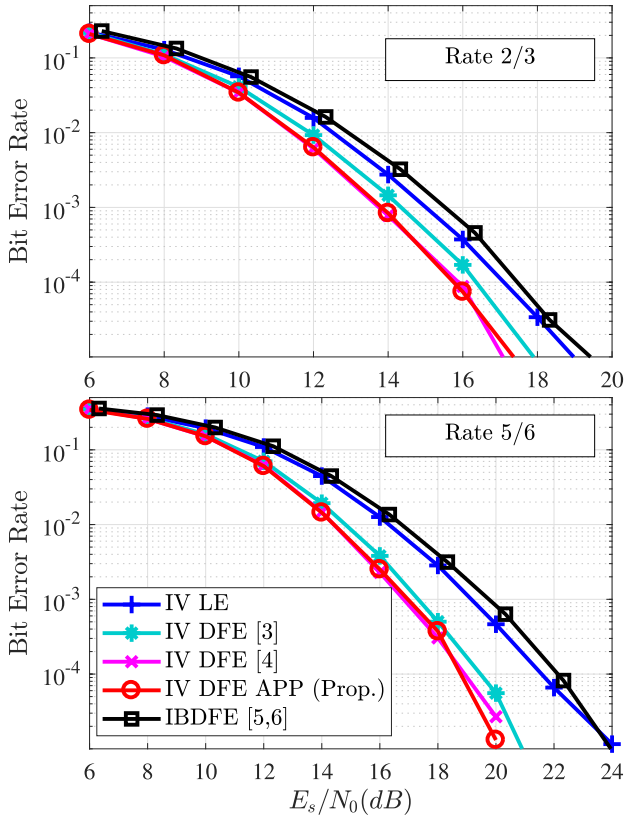

FIGURE 14. BER comparison vs. FDE in a uniformly distributed 10-tap Rayleigh fading channel for 1 turbo iteration.

for circular transmission. This causes a loss of spectral efficiency, which can be more or less significant depending on the delay spread of the channel. Moreover, when using an FDE, interference-cancellation has to be carried out in a parallel-schedule, whereas FIR structure use serial decision feedback, on top of the decoder feedback. Hence FIR structures have likely better computational complexity trade-off for systems that need to exploit the benefits of serial decision feedback, such as the considerable energy-efficiency gains in high data rate applications. Finally, when the channel is no longer quasi-static, neither FDE or FIR IV DFE structures are able to cope with the time-selectivity of the channel, and FIR TV DFE structures [1] or time-domain block filter-bank structures are needed [27].

For comparing these structures with numerical results, we first consider their uncoded BER performance in Proakis C, as illustrated in Figure 13. In this case, we compare the uncoded original IBDFE's [5] performance across the number of iterations N_{si}, in the Proakis C channel, with 8-PSK and $K = 256$. It is seen that while IBDFE manages to have a lower error-rate, at low SNR, it is unable to recover the full channel diversity, unlike IV and TV DFE structures. Moreover, FDE structures are penalized by approximately 0.1 dB, due to cyclic prefixing.

The turbo-equalization performance of IBDFE, in coded systems is given in Figure 12, for the same rate-2/3 and rate-5/6 convolutionally coded systems as in the previous subsection. IBDFE of [5] becomes a frequency domain linear equalizer [6] in the turbo context, which uses the soft decoder feedback for equalization, and hence faces the similar limitations to the FIR IV LE.

Next, we look into the turbo equalization performance of these structures in a more realistic Rayleigh fading channel, with $L = 10$, and uniformly distributed, symbol-spaced power-delay profile. In Figure 14, rate-2/3 and rate-5/6 convolutionally coded systems with $K = 128$ are compared for 1 turbo-iteration. FIR DFE solutions have significant advantage over IBDFE and FIR LE, with the proposed DFE and the receiver of [4] exhibiting lower bit error rates. The performance differences between FIR DFEs is lower, as most realizations of the random quasi-static fading channel are not significantly frequency-selective.

In conclusion, while the FDE structure have a significant computational complexity advantage, they are outperformed by FIR structures which manage to exploit serial decision feedback, and without being penalized by cyclic prefixing overhead. IV DFE hence provide an alternative solution for equalization in high throughput applications, with improved decoding performance, at the expense of some additional computational costs.

V. CONCLUSION

This paper carries out an original approach to the design of turbo DFE receivers with static filters, through the use of online prediction, based on semi-analytic performance prediction techniques as used in physical layer abstraction methods. Due to the lack of a closed-form solution for such receivers, various heuristics are used throughout the literature. However, discussion on the optimality of such approaches was lacking and it is one of the contribution of this paper.

Here, semi-analytical performance prediction of exact time-varying turbo DFE with dynamic filters is exploited to derive static DFE filters. This approach has been carried out for DFE with APP-based or EP-based soft feedback and their detection performance has been evaluated in various configurations. This framework could also be applied to self-iterated FIR DFE [1] for further improved performance, by updating anti-causal variances with causal EP variance of the last self-iteration.

Our analysis shows that significant complexity savings can be achieved with respect to TV DFE, while offering reasonably close performance. Moreover, our method is compatible with any constellation, and spectrally efficient on a large interval of coding rates, with or without turbo-iterations. The proposed structure is also shown to be a good alternative to low-complexity frequency domain turbo equalizers (IBDFE) as they can decode with lower received signal strength for high data rate applications, without being penalized by cyclic prefixing overhead, but at the cost of increased filter computation complexity.

REFERENCES

[1] S. Şahin, A. M. Cipriano, C. Poulliat, and M. Boucheret, "Iterative equalization with decision feedback based on expectation propagation," *IEEE Trans. Commun.*, vol. 66, no. 10, pp. 4473–4487, Oct. 2018.
[2] M. Tuchler and A. C. Singer, "Turbo equalization: An overview," *IEEE Trans. Inf. Theory*, vol. 57, no. 2, pp. 920–952, Feb. 2011.
[3] H. Lou and C. Xiao, "The soft-feedback ISI canceller-based turbo equalizer for multilevel modulations," *Int. J. Wireless Inf. Netw.*, vol. 21, no. 1, pp. 68–73, Mar. 2014.
[4] J. Tao, "On low-complexity soft-input soft-output decision-feedback equalizers," *IEEE Commun. Lett.*, vol. 20, no. 9, pp. 1737–1740, Sep. 2016.
[5] N. Benvenuto, R. Dinis, D. Falconer, and S. Tomasin, "Single carrier modulation with nonlinear frequency domain equalization: An idea whose time has come—Again," *Proc. IEEE*, vol. 98, no. 1, pp. 69–96, Jan. 2010.
[6] M. Tüchler and J. Hagenauer, "Linear time and frequency domain turbo equalization," in *Proc. IEEE 54rd Veh. Technology Conf.*, vol. 4, Nov. 2001, pp. 2773–2777.
[7] S. Jeong, "Low complexity turbo equalizations and lower bounds on information rate for intersymbol interference channels," Ph.D. dissertation, Univ. Minnesota, Minneapolis, MN, USA, Oct. 2011.
[8] C. A. Belfiore, "Decision feedback equalization," *Proc. IEEE*, vol. 67, no. 8, pp. 1143–1156, Aug. 1979.
[9] M. Tuchler, R. Koetter, and A. Singer, "Turbo equalization: Principles and new results," *IEEE Trans. Commun.*, vol. 50, no. 5, pp. 754–767, May 2002.
[10] S. Jeong and J. Moon, "Turbo equalization based on bi-directional DFE," in *Proc. IEEE Int. Conf. Commun.*, May 2010, pp. 1–6.
[11] R. Lopes and J. Barry, "The soft-feedback equalizer for turbo equalization of highly dispersive channels," *IEEE Trans. Commun.*, vol. 54, no. 5, pp. 783–788, May 2006.
[12] T. P. Minka, "A family of algorithms for approximate Bayesian inference," Ph.D. dissertation, MIT, Chennai, Indian, Jan. 2001.
[13] D. Li, Y. Wu, J. Tao, and M. Zhu, "Performance analysis and improvement for VAMP soft frequency-domain equalizers," *IEEE Access*, vol. 7, pp. 42495–42506, 2019.
[14] J. Balakrishnan, "Mitigation of error propagation in decision feedback equalization," M.S. thesis, Dept. Elect. Comput. Eng., Cornell Univ., Urbana-Champaign, IL, USA, 1999.
[15] R. Visoz, A. O. Berthet, and M. Lalam, "Semi-analytical performance prediction methods for iterative MMSE-IC multiuser MIMO joint decoding," *IEEE Trans. Commun.*, vol. 58, no. 9, pp. 2576–2589, Sep. 2010.
[16] M. Sabbaghian and D. Falconer, "An analytical approach for finite block length performance analysis of turbo frequency-domain equalization," *IEEE Trans. Veh. Technol.*, vol. 58, no. 3, pp. 1292–1301, Mar. 2009.
[17] X. Yuan, Q. Guo, X. Wang, and L. Ping, "Evolution analysis of low-cost iterative equalization in coded linear systems with cyclic prefixes," *IEEE J. Sel. Areas Commun.*, vol. 26, no. 2, pp. 301–310, Feb. 2008.
[18] S. T. Brink, "Designing iterative decoding schemes with the extrinsic information transfer chart," *AEU Int. J. Electron. Commun.*, vol. 54, no. 6, pp. 1–10, Jan. 2000.
[19] M. Fu, "Stochastic analysis of turbo decoding," *IEEE Trans. Inf. Theory*, vol. 51, no. 1, pp. 81–100, Jan. 2005.
[20] A. Ibing and H. Boche, "On predicting convergence of iterative MIMO detection-decoding with concatenated codes," *IEEE Trans. Veh. Technol.*, vol. 59, no. 8, pp. 4134–4139, Oct. 2010.
[21] S. Jeong and J. Moon, "Self-iterating soft equalizer," *IEEE Trans. Commun.*, vol. 61, no. 9, pp. 3697–3709, Sep. 2013.
[22] J. Hagenauer, "The EXIT chart—Introduction to extrinsic information transfer in iterative processing," in *Proc. IEEE 12th Eur. Signal Process. Conf.*, Sep. 2004, pp. 1541–1548.
[23] D. Arnold, H.-A. Loeliger, P. Vontobel, A. Kavcic, and W. Zeng, "Simulation-based computation of information rates for channels with memory," *IEEE Trans. Inf. Theory*, vol. 52, no. 8, pp. 3498–3508, Aug. 2006.
[24] L. Bahl, J. Cocke, F. Jelinek, and J. Raviv, "Optimal decoding of linear codes for minimizing symbol error rate," *IEEE Trans. Inf. Theory*, vol. IT-20, no. 2, pp. 284–287, Mar. 1974.
[25] B. Ning, R. Visoz, and A. O. Berthet, "Extrinsic versus a posteriori probability based iterative LMMSE-IC algorithms for coded MIMO communications: Performance and analysis," in *Proc. IEEE Int. Symp. Wireless Commun. Syst.*, Aug. 2012, pp. 386–390.
[26] N. Souto, R. Dinis, A. Correia, and C. Reis, "Interference-aware iterative block decision feedback equalizer for single-carrier transmission," *IEEE Trans. Veh. Technol.*, vol. 64, no. 7, pp. 3316–3321, Jul. 2015.
[27] G. Kaleh, "Channel equalization for block transmission systems," *IEEE J. Sel. Areas Commun.*, vol. 13, no. 1, pp. 110–121, Jan. 1995.

SERDAR ŞAHİN was born in Ankara, Turkey, in 1992. He received the M.Sc.Eng. degree in control systems and electronics engineering from the INSA de Toulouse, University of Toulouse, France, in 2015. He is currently pursuing the Ph.D. degree in digital communications with IRIT–ENSEEIHT, Toulouse, and also with Thales Communications and Security, Gennevilliers. His main research interests include iterative receiver design, practical cooperative transmission schemes, and PHY layer abstraction.

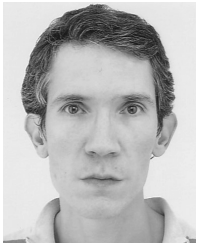

ANTONIO MARIA CIPRIANO was born in Padova, Italy, in 1976. He received the Laurea degree in telecommunications engineering from the University of Padova, Italy, in 2000, and the Ph.D. degree in digital communications jointly from the University of Padova and the Ecole Nationale Supérieure des Télécommunications (ENST) Paris, France, in 2005. In 2001, he was a Young Engineer with Eutelsat, France, for eight months. From 2005 to 2007, he held two Postdoctoral Researcher positions at ENST, Paris, and Orange Labs. In 2007, he joined as a Digital Communication Engineer with Thales Communication and Security. He was involved in several national and international research projects on 4G and 5G communication systems. He is currently involved in research about PHY layer abstractions, relaying for ad hoc mobile networks, and advanced receiver design. His main research interest includes in the broad area of digital communication systems.

CHARLY POULLIAT received the M.Sc.Eng. degree in electrical engineering from the Ecole Nationale Supérieure de l'Electronique et de ses Applications (ENSEA), Cergy-Pontoise, France, in 2001, and the M.S. degree in image and signal processing, the Ph.D. degree in electrical and computer engineering, and the Habilitation degree from the University of Cergy-Pontoise, France, in 2001, 2004, and 2010, respectively. From 2004 to 2005, he was a Postdoctoral Researcher with the UH Coding Group, University of Hawaii at Manoa, Honolulu, HI, USA, supervised by Prof. M. Fossorier. In 2005, he joined the Signal and Telecommunications Department, Engineering School ENSEA, as an Assistant Professor. Since 2011, he has been a Professor with the National Polytechnic Institute of Toulouse (INP-ENSEEIHT), University of Toulouse. He is also with the Signal and Communications Group, CNRS IRIT Laboratory. His research interests include signal processing for digital communications, waveform design, channel coding, iterative system design, and optimization.

MARIE-LAURE BOUCHERET received the M.Sc.Eng. degree in electrical engineering from ENST Bretagne, Brest, France, in 1985, the Ph.D. degree in digital communications from TELECOM ParisTech, in 1997, and the Habilitation à diriger des recherches degree from the INPT University of Toulouse, in 1999. From 1985 to 1986, she was a Research Engineer with the French Philips Research Laboratory (LEP). From 1986 to 1991, she was an Engineer with Thales Alenia Space, first as a Project Engineer (TELECOM II program), then as a Study Engineer with the Transmission Laboratory. From 1991 to 2005, she was with TELECOM ParisTech, first as an Associated Professor, then as a Professor. Since 2005, she has been a Professor with the National Polytechnic Institute of Toulouse (INP-ENSEEIHT), University of Toulouse. She is also with the Signal and Communication Group, IRIT Laboratory. Her fields of interest are signal processing for communication and satellite communications.